CONF-970302--4 SAND 97-0972C

SURFACE CHARGING OF PHOSPHORS AND ITS EFFECTS ON CATHODOLUMINESCENCE AT LOW ELECTRON ENERGIES

C. H. SEAGER, W. L. WARREN, and D. R. TALLANT
Sandia National Laboratories, Albuquerque, NM, 87185, chseage@sandia.gov

RECEIVED
MAY 0 8 1997
OSTI

ABSTRACT

Measurements of the threshold for secondary electron emission and shifts of the carbon Auger line position have been used to deduce the surface potential of several common phosphors during irradiation by electrons in the 0.5 - 5.0 keV range. All of the insulating phosphors display similar behavior: the surface potential is within ±1 V of zero at low electron energies. However, above 2-3 kV it becomes increasingly negative, reaching hundreds of volts within 1 keV of the turn-on energy. The electron energy at which this charging begins decreases dramatically after Coulomb aging at 17 $\mu A/cm^2$ for 30-60 min.. Measurements using coincident electron beams at low and high electron energies to control the surface potential were made to investigate the dependence of the cathodoluminescence (CL) process on charging . Initially, the CL from the two beams is identical to the sum of the separate beam responses, but after Coulomb aging large deviations from this additivity are observed. These results indicate that charging has important, detrimental effects on CL efficiency after prolonged e-beam irradiation. Measurements of the electron energy dependence of the CL efficiency before and after Coulomb aging will also be presented, and the implications of these data on the physics of the low-voltage CL process will be discussed.

INTRODUCTION

Recent attention has been focussed on the suitability of conventional CRT phosphors for field emission displays[1] (FED) operating at electron accelerating voltages below 5kV. Most phosphors display a severe reduction in their cathodoluminescence (CL) efficiency at voltages below this value[2], apparently because electron-hole or plasmon de-excitation at surface states of either extrinsic or intrinsic origin becomes important. Since most of the surface-related pathways for energy loss are expected to be non-radiative, sizable decreases in the CL efficiency might be anticipated. In fact, most phosphors display[2] a CL efficiency which essentially drops linearly to zero below an electron excitation energy of 5 kV.

A second concern raised by low voltage operation is the concentration of excitation energy in an increasingly smaller volume as the electron range shrinks at low beam energies. This concentration of power might be expected to give rise to more severe Coulomb aging effects. In this case the drop in CL efficiency at lower beam energies exacerbates this problem.

Given these facts it is clear that a fundamental understanding of the CL process at low beam energies will be needed to develop robust and efficient phosphors for FED applications. Here we explore two issues which might become important for these materials: surface charging during electron beam exposure and degradation of the luminescence due to Coulomb loading.

MASTER
DISTRIBUTION OF THIS DOCUMENT IS UNLIMITED

EXPERIMENT

Four phosphors, ZnS:Ag, $SrGa_2S_4$:Eu, ZnO:Zn, Y_2O_3:Eu, and two bulk insulators, KCl and a-SiO_2 were characterized in this study. Screens of the phosphor powders were fabricated by sedimenting particles from a solution of magnesium nitrate hexahydrate and isopropanol onto ~1 cm^2 Au foil. Phosphor particle diameters were typically 1-10μm, and the typical screen had a layer of 5-10 particles in depth. ~ 1 mm thick plates of the bulk insulators were glued onto the same foils. These screens were mounted on a carousel in an ion pumped vacuum system which had base pressures in the range of 9-15 x 10^{-5} Pa. CL measurements were made with 2-3 mm diameter beam spots of one or two electron guns capable of operating in the range of 0.1 to 5 kV. The spectral variation of the CL was measured with a fiber-optic-coupled spectrometer interfaced to a personal computer.

The electrical transport properties of the four phosphor powders studied here have not been characterized extensively. The ZnO powder was reduced at high temperatures in an H_2-rich environment yielding a shallow donor/carrier concentration of ~ 3 x 10^{17} cm^{-3}. Using an electron mobility of 100 cm^2/V.sec we calculate that the intragrain conductivity is ~5 mhos/cm, but grain-to-grain resistance may play a significant role in limiting currents to the screen backing foil. The other three phosphors are all wide band gap insulators with no incorporated shallow dopants; as a consequence they have unmeasurably low free carrier densities.

To determine V_S, the surface potential of the phosphor screens, a conventional Auger spectrometer was employed with an axial e-gun and a single pass cylindrical mirror analyzer (CMA). The samples were typically positioned 2-3 mm from the CMA entrance, and the spectrometer parameters were carefully tuned to maximize signal to noise at the low beam current densities used (typically less than 4 μA/cm^2). Two types of spectra were taken to track the phosphor surface potential: 1. measurements of the secondary electron (SE) spectra at relatively low electron energies (0-25 eV for an uncharged surface). 2. Measurements of the carbon KLL Auger electron peak at 260-290 eV. This latter signature was by far the cleanest Auger peak measurable because of the substantial adventitious hydrocarbon layer seen on all surfaces under these vacuum conditions.

Because the sample carousel and the screens (the Au foil backplane) could be electrically isolated from the rest of the system, we were able independently bias the screens and determine the amount of current flowing to system ground with a Keithley 616 electrometer. By adjusting this collection bias, V_{cb}, to a large positive value (40-80V), most of the secondary electrons could be collected on the back of the screen and the carousel. Thus the beam current minus the backscattered fraction could be determined. By biasing the screens and carousel negatively to prevent collection of secondaries we could also study the fraction of current flowing through the phosphor particles as well as the dependence of the surface potential on the field in the phosphor. This data is useful in analyzing the nature of the internal phosphor electric fields.

RESULTS

Typically both SE and Auger spectra were collected on all samples. If e-beam exposure was kept to a minimum, the surface potentials determined from both spectroscopies were essentially identical within the accuracy of our measurements (~ ± 1 V). Figure 1 shows SE spectra taken on ZnO:Zn with beam energies ranging from 0.5 to 3 keV. On this conductive phosphor, there are only small shifts of the threshold for secondary electron emission. The trend is for the surface to become 1-2 volts more negative as the e-beam energy is raised from 0.5 to 3 keV.

DISCLAIMER

This report was prepared as an account of work sponsored by an agency of the United States Government. Neither the United States Government nor any agency thereof, nor any of their employees, makes any warranty, express or implied, or assumes any legal liability or responsibility for the accuracy, completeness, or usefulness of any information, apparatus, product, or process disclosed, or represents that its use would not infringe privately owned rights. Reference herein to any specific commercial product, process, or service by trade name, trademark, manufacturer, or otherwise does not necessarily constitute or imply its endorsement, recommendation, or favoring by the United States Government or any agency thereof. The views and opinions of authors expressed herein do not necessarily state or reflect those of the United States Government or any agency thereof.

DISCLAIMER

Portions of this document may be illegible in electronic image products. Images are produced from the best available original document.

In contrast to the ZnO:Zn, where currents measured through the phosphor material to the Au foil backplane were 40-60% of incident beam values, currents for the other three types of phosphor powder were zero within our noise level, suggesting that they are excellent insulators. Screens made from these other phosphors also showed much larger negative shifts in surface potential, as inferred from the (adventitious) C Auger peak and SE threshold kinetic energies. Some of these data are shown in Figure 2. As the surface potential became more negative we observed that the C Auger KLL derivative peak weakened and became smeared out, and the onset of the SE threshold became more difficult to determine as these spectra broadened also. We inferred from this behavior that the surfaces of these phosphor screens were charging inhomogeneously, a reasonable result for a surface composed of areas of different crystallographic orientations and varied beam impingement angles. Extended exposure at higher beam currents causes more pronounced negative surface charging. V_s begins to drop (become negative) at lower beam energies and the onset of charging is more abrupt. Figure 3 illustrates these effects for $SrGa_2S_4$:Eu. Similar results were observed for Y_2O_3 and ZnS. This type of surface charging response is not peculiar to screens made from powdered insulators; we observed[3] that bulk samples of insulating materials like a-SiO_2 and KCl also display similar behavior (not shown).

Coulomb aging protocols also markedly affect the CL of these phosphors, particularly at low beam energies. Figure 4 shows data for Y_2O_3:Eu aged at 1.5 keV; notice that the normalized beam energy dependence of the CL becomes non-monotonic in beam energy after several hours of aging. This change in sign of the slope or "rollover" of the CL surface above 2 keV was also seen for the $SrGa_2S_4$:Eu, and, to a lesser extent, for the ZnS:Ag. We believe that this feature is due to a particularly simple feature of the aging process which will be discussed below.

In addition to the effects of varying the electron beam energy, we could also vary the surface potential of our phosphor screens by adjusting the potential of the metal plates on which they were deposited. For good conductors the surface potential is pinned at the power supply bias. This is observed on screens of ZnO:Zn. However, a different result is found when this experiment is performed on screens of the three insulating phosphors. This is illustrated in Figure 5 for Y_2O_3:Eu. At beam energies below 2 keV where no surface charging is observed, the Auger peak position shifts linearly with collection bias as expected, but the slope of this plot is close to 1/2, quite different than the unity value observed for conductive samples. As the beam energy is increased above the charging threshold, the slopes of these plots gradually increase as the sample charges up. This collection bias dependence was also seen in SE threshold measurements, although SE data could only be collected at negative or slightly positive surface potentials due to the low energies of these species. This effect was also seen[3] on our bulk insulating samples (not shown). Below we will show that this data implies the existence of space charge below the insulator surface, even at low electron beam energies.

Finally, we utilized dual electron beam experiments to probe the effects of surface charging on the CL response. These measurements were conducted with one electron gun at normal incidence and the other impinging on the same spot at 30° from normal. In all cases we restricted the total electron current densities to values where the individual beam CL response was linear, so that differences between single and dual beam CL would be expected to vanish if the response to each beam was ***independent of the presence of the other beam***. CL data obtained with this dual electron beam arrangement are shown in Figure 6 for several beam energies of the normal-axis (low energy) gun. In these studies the off-axis gun was operated at 4 keV. The quantity plotted in this Figure is the difference between the sum of the observed individual responses of each gun and the response to both beams impinging simultaneously; it is

normalized by the high energy (4 keV) CL response. In this plot the dependence on the energy of the low energy electron beam vanishes for all but the 350 eV $SrGa_2S_4$:Eu data point. For all but the lowest beam energy employed, it appears that a second beam enhances the high energy beam CL by a constant fraction over the 500-950 keV energy range; arguments will be offered below which suggest that the low energy beam pins the surface potential at zero over this range. Data on the other insulating phosphors show a decrease in this enhancement at low energies as well[3] (not shown) It is possible that the surface potential pinning is prevented at low beam energies because the beam energy drops below the average value of V_S, preventing it from impinging on the sample. Finally, we note that no enhancement effects are seen for the ZnO:Zn in Figure 6; this is expected from the minimal surface potential shifts observed in the electron spectroscopy data on this material (Fig. 1).

Experiments have also been performed to examine the Coulomb aging effect. We observe that extended beam exposure always leaves our screens slightly darkened when viewed in reflected light. Reflection photometry as well as measurements of the spectral shifts of the emitted cathodoluminescence (data not shown) indicate that a surface layer of increasing opacity forms with electron exposure[4]. We have performed Raman spectroscopy measurements[4] on these exposed surfaces; some of this data is shown in Figure 7. It shows that the aged area contains material with the Raman signature of microcrystalline graphite[5,6]. These data suggest that we are cracking the hydrocarbon/CO/CO_2 contaminant layer that is always present under these vacuum conditions. Continuous accretion of carbon during electron beam exposure at high current densities is n effect[7] well known to electron microscopists, and it could cause a decline in CL particularly at low voltages where the end-of-range for electrons is only hundreds of angstroms. We have not been able to see any measurable vacuum pressure dependence of the Coulombic aging process over the range from 2.7×10^{-5} to 2.7×10^{-3} Pa, even at beam currents as high as 160 $\mu A/cm^2$. While these results might, at first glance, cast doubt on the applicability of this mechanism, it is possible that the rate of beam induced polymerization is low, and that species arrival from the ambient is not the rate-limiting step[8]. There is also the issue of whether hydrocarbons could be continously refreshed in the exposed area by a surface diffusion mechanism, but we think that the large spot sizes in our experiment make this somewhat unlikely.

CONCLUSIONS

A number of past studies have addressed the issue of insulator charging during e-beam exposure[9-16]. Figure 8 shows generic curves of secondary, δ, and backscattered electron yield, η, as a function of the arriving electron energy. For a typical material, $\delta+\eta$ possesses two crossovers where the fraction of electrons leaving the material is unity. If no currents flow to ground through the insulator, some changes in these curves or in the arrival energy must occur to accomodate steady state at other electron energies. For instance, if a sample with zero surface potential is in steady state at E_2, and this electron energy is increased by an increment Δ, steady state might be re-established if the surface potential, V_S, changed from 0 to $-\Delta$. This would leave the arrival energy of the electrons incident on the surface unchanged. This simple scenario might occur if δ were only a function of arrival energy and not sensitive to the internal field in the specimen and the vacuum field just outside the sample[13,16]. The internal sample fields are established by external voltages impressed on the system and by the configuration of any space charge caused by the irradiation conditions. The vacuum field plays a role because of the requirement that the dielectric displacement vector must be continuous.

Several investigators[16,17] have pointed out that this simple shift of the surface potential is not always observed; given the complicated nature of this problem, this result should not surprise us. Indeed, the surface potentials plotted in Figures 2 and 3 do not have a slope of unity above the point where they start to increase markedly; the observed rate of change (of negative surface potential) is much slower. The behavior below the charging threshold is interesting as well. It has been suggested that beam energies between E_1 and E_2 might result in a large enough positive shift in the surface potential that recapture of emitted secondaries would serve to stabilize the surface potential[15,16]. Two features of our data are inconsistent with this mechanism. First, judging from secondary electron curves like those shown in Figure 1, V_S would have to be at least several volts positive to recapture a significant fraction of emitted secondaries. This is not observed. Secondly, the plots of Carbon Auger peak energy versus V_{cb} have essentially the same slope from -20V to + 20V, even when V_S is substantially positive (the lowest plot in Figure 5). So the functional dependence of V_S on collection bias does not change, even when the surface goes from capturing to repelling emitted secondaries. This suggests that recapture effects (at least in this bias range) are not the dominant effect which keeps V_S near zero at low beam energies. Somehow secondary emission is ***internally*** regulated to make $\delta+\eta$ equal to unity.

How does this come about? We believe that the collection bias dependence of V_S shown in Figure 5 provides insight into this problem. If one regards the layer of phosphor particles as a dielectric material of uniform thickness t_i with (relative) dielectric constant ε , then it can be shown that the fraction of the collection bias dropped across the phosphor material is ~ $t_i/(\varepsilon t_g)$, where t_g is the vacuum gap (~1 cm). This is true *if no excess charge* resides in the insulator or at the vacuum/insulator interface. In our experiment $t_i/t_g<<1$, so that most of the collection bias should be dropped across the vacuum gap, in contradiction to the results in Figure 5. These experimental results indicate that space charge must be present in both the bulk insulators and the phosphors during electron irradiation. What type of space charge distribution might we expect? Cazaux has hypothesized[13,16] that negative space charge might be present near the end of range for electrons and positive charge near the insulator surface. We think that this is a reasonable suggestion. To make a realistic calculation of the expected space charge would require a transport code which includes the e-h pair generation function due to excitation from the incident e-beam, mobilities and recombination lifetimes for both electrons and holes, and the inclusion of the internal electric fields set up by the presence of these species. This is a formidable task, made even more difficult by the present lack of knowledge of electron and hole transport parameters in many of these phosphors. However, certain features of the electrostatic solutions for this problem can be exploited to give some general guidelines for the simplest space charge arrangement that is consistent with the data. This is discussed in more detail elsewhere[3]. The general conclusion of these arguments is that both positive and negative regions exist near the insulator surface. It is also likely that the width of these regions must be dependent on the insulator electric field. In our experiment, this field is a function of both the external power supply bias and the excess charges generated by the incident electron beam.

The impact of these beam-induced space charge regions on the magnitude of secondary electron emission δ could be substantial. If potential differences of 5-10 V occur in the ~50Å region just below the insulator surface, SE emission will be strongly influenced[18]. Fields this strong are close to the bulk breakdown strength, and indeed beam-induced breakdown has been reported for a number of insulating materials[17]. These observations should be regarded as *a priori* evidence for these large fields. We suggest that the nearly zero values of V_S observed by us at low beam energies (where δ is expected to be > unity) are a result of internal fields that

partially retard SE emission. But when the beam energy exceeds E_2, the electric fields which push electrons out of the material must increase, enhancing the emission process and stabilizing δ at the value of $1-\eta$. The reduction in arrival energy caused by more negative surface potentials could play a role in raising δ, but this does not appear to be the dominant effect.

The two beam CL experiments show large enhancement effects after Coulomb aging, but almost none before. Since the amount of surface charging is also much bigger after aging (see Fig. 4), this suggests that the enhancements are due to charging effects. SE coefficients are largest at these low beam energies, so it seems reasonable that the primary effect of adding a low energy beam is to reduce the negative V_S values expected at 4 keV. The first order effect of a large negative V_S is to reduce the electron arrival energy. The dependence on arrival energy, E, of the high voltage gun response, R_{HE}, is:

$$R_{HE} \alpha E^2 \qquad (2)$$

(this comes from the data on these same phosphors in reference 3). Then the change in CL response after a change of arrival energy, $\Delta E=\Delta V_S$, will be:

$$\Delta R_{HE}/R_{HE} = 2\,\Delta V_S/E \qquad (3)$$

So for instance the ~15% enhancement seen in Figure 6 for Y_2O_3:Eu would require a change of ~7% in the arrival energy at 4 keV. This is would indicate that the low energy beam has made the surface potential more positive by ~ 300V at 4 keV. Because of inhomogeneous charging, our electron spectroscopy studies cannot follow the evolution of V_S above 150-200V, but a (negative) surface potential of this magnitude does not seem unreasonable considering the beam energy dependence in Figures 2 and 3. The 350V data of Figure 6 and other experiments (not shown) are also consistent with V_S values greater than 300V. While these arguments are qualitatively reasonable, they do not preclude the existence of other effects in the two beam experiments.

We believe that the enhancement of charging seen after aging is due to the accretion of graphitic carbon on the phosphor surfaces. Prior work has shown that thin metallic layers deposited on insulators will charge up during 2-4 keV beam irradiation, even when an adjacent, uncoated insulator surface does not[16]. This effect is presumably due to the low secondary electron emission coefficients of typical metals (a property shared by graphite). Based on our dual beam studies, it is almost certain that charging causes the "rollover" at higher energies seen in the CL data in Fig. 4.

Figure 4 shows that extended beam exposures decrease CL even more dramatically at low electron energies. Since we have never observed charging in aged samples below 1 keV, it is clear that Coulomb aging effects are not wholly due to enhanced charging. What are the mechanisms that reduce the low voltage CL? One might first ask why the CL efficiencies are such a strong function of electron beam energy ***before aging***. Leamy has modeled beam excitation[19] near a surface possessing various recombination velocities, S. Not surprisingly, he finds that as S tends toward infinity, the steady state concentration of electron-hole pairs decreases strongly as the electron range drops. So, it is likely that strong surface recombination exists before aging and that that extensive Coulomb exposure could, either a) create more radiationless recombination pathways at the surface, or b) alter the near surface density of these sites, or c) change the local electric fields that drive the motion of electrons and holes. Another important effect that should not be overlooked is the attenuation of incoming electrons by the

contamination overlayer. Our optical studies suggest that this layer may be at least 100Å thick after the aging sequence shown in Figure 4. Since the penetration depth of 500eV electrons is only ~140Å in phosphors like ZnS[4,21], many of the incoming electrons stop in this graphitic material. An accurate accounting of the CL changes after aging clearly depends on careful estimates of the thickness and stopping power of these beam-induced contaminants. This is a subject for future study.

ACKNOWLEDGEMENTS

The authors would like to thank Jonathan Campbell for assistance with the experimental measurements and R. Anderson, J. Houston, D. Joy, and T. Headley for useful discussions about the interpretation of the data. N. Yocum of the David Sarnoff Research Center and A. Vecht of the Univ. of Greenwich were kind enough to supply some of the phosphor materials. This work was supported by DARPA and by the United States Department of Energy under Contract DE-AC04-94AL85000. Sandia is a multiprogram laboratory operated by Sandia Corporation, a Lockheed Martin Company, for the United States Department of Energy.

REFERENCES

1. J. E. Jaskie, MRS Bulletin. **21**, 59 (1996).
2. L. Ozawa, in *Cathodoluminescence* (Kodansha, Tokyo, 1990).
3. C. H. Seager, W. L. Warren, and D. Tallant, to be published in the Journal of Applied Physics.
4. C. H. Seager, D. Tallant, and W. L. Warren, submitted to the Journal of Applied Physics.
5. F. Bart, M. J. Guittet, M. Henriot, N. Thromat, M. Gautier, and J. P. Duraud, J. Electron Spectros.**69**, 245 (1994).
6. I. S. Gilmore and M. P. Seah, Surf. and Interf. Analy. **23**, 191 (1995).
7. J. J. Hren in *Principles of Scanning Microscopy* ed. by D. C. Joy, A. L. Romig, and J. I. Goldstein (Plenum, New York, 1986), p.353.
8. P. Holloway, private communication.
9. F. Bart, M. J. Guittet, M. Henriot, N. Thromat, M. Gautier, and J. P. Duraud, J. Electron Spectros.**69**, 245 (1994).
10. I. S. Gilmore and M. P. Seah, Surf. and Interf. Analy. **23**, 191 (1995).
11. G. Slodzian, Optik 77, 148 (1987).
12. D. Decroupet, M. Liehr, P. A. Thiry, J. J. Pireaux, and R. Caudano, J. Vac. Sci. Technol. **A4**, 1304 (1986).
13. J. Cazaux, J. Appl. Phys. **59**, 1418 (1986).
14. J. Cazaux, Inst. Phys. Conf. Series No. 93, **2**, 375 (1988).
15. J. Cazaux and C. Le Gressus, Scanning Microsc.**5**, 17 (1991).
16. J. Cazaux and P. Leheude, J. Electron Spectroscopy and Rel. Phenom. **59**, 49 (1992).
17. D. C. Joy and C. S. Joy, MICRON **27**, 247 (1996).
18. G. F. Amelio, J. Vac. Sci. Technol. 7, 593 (1970).
19. H. J. Leamy, in *Physical Electron Microscopy*, ed. by O. C. Wells, K. F. J. Heinrich, and D. E. Newbury (Van Nostrand Reinhold, New York, 1981).
20. P. H. Hoff and T. E. Everhart, IEEE Trans Elect. Devices **ED17**, 452 (1970).

FIGURE CAPTIONS

Figure 1. Secondary electron emission spectra measured for ZnO:Zn as a function of electron beam energy from 0.5 keV to 3 keV (in 500V steps). Only small shifts of the SE threshold are seen for this conductive phosphor.

Figure 2. SE thresholds and carbon Auger line peak positions as a function of electron beam energy before Coulomb aging for three insulating phosphors.

Figure 3. C Auger kinetic energy as a function of e-beam energy for $SrGa_2S_4$:Eu before and after Coulomb aging at 1.5 keV, 10$\mu A/cm^2$.

Figure 4. The change in CL intensity as a function of e-beam energy during Coulomb aging of Y_2O_3:Eu at 1500 eV and 20 $\mu A/cm^2$. The CL intensity is normalized by the starting (unaged) values. Other experiments suggest that the negative slope of the CL surface with beam energy at long exposures is a result of negative charging of the phosphor surface.

Figure 5. The dependence of the C Auger peak kinetic energy on collection bias for Y_2O_3:Eu measured before Coulomb aging. Note that the abscissa plots -Vcb. S values are the slopes of the least squares fit straight lines.

Figure 6. The two-beam enhancement divided by the high energy beam CL response for all four phosphors versus the energy of the on-axis electron gun. Open symbols are data taken at 4 keV, 1.4 $\mu A/cm^2$, filled symbols data at 4 keV, 2.8$\mu A/cm^2$. These samples were Coulomb aged at 1.5 keV before this measurement. Over most of the gun voltage range, this enhancement fraction is essentially a constant for each phosphor.

Figure 7. Raman spectra for aged and unaged portions of a screen of Y_2O_3:Eu. The broad bands near 1350 and 1600 cm^{-1} are characteristic of nanocrystalline graphite. The narrow peaks at 1470 cm^{-1} may be due to luminescence from the Eu^{3+} activators.

Figure 8. The variation of the backscattered, η, and secondary emission, δ, electrons from a typical material. The two crossover energies where the sum of these two fractions is unity are labelled.

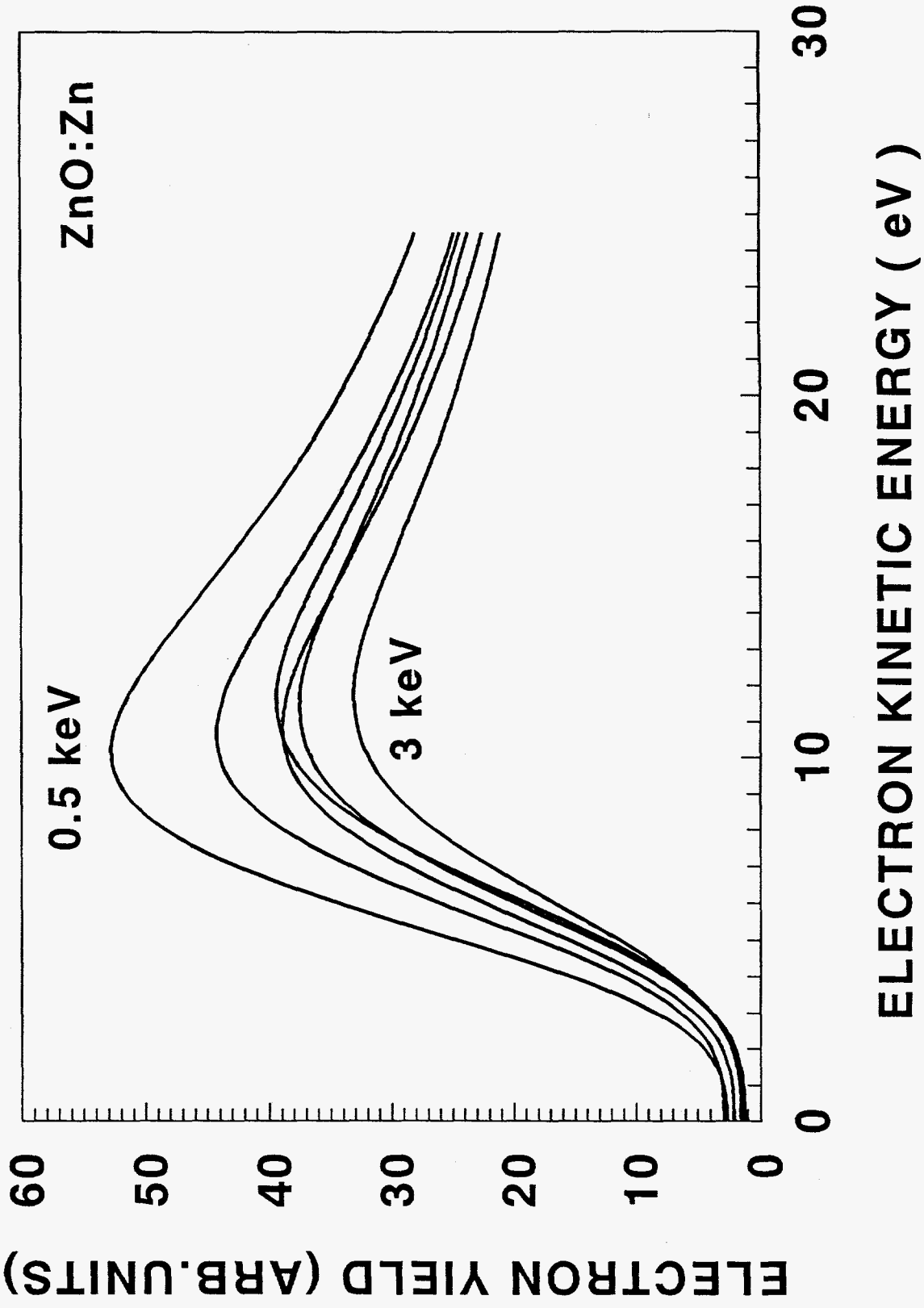

Fig. 1 Seager et al.

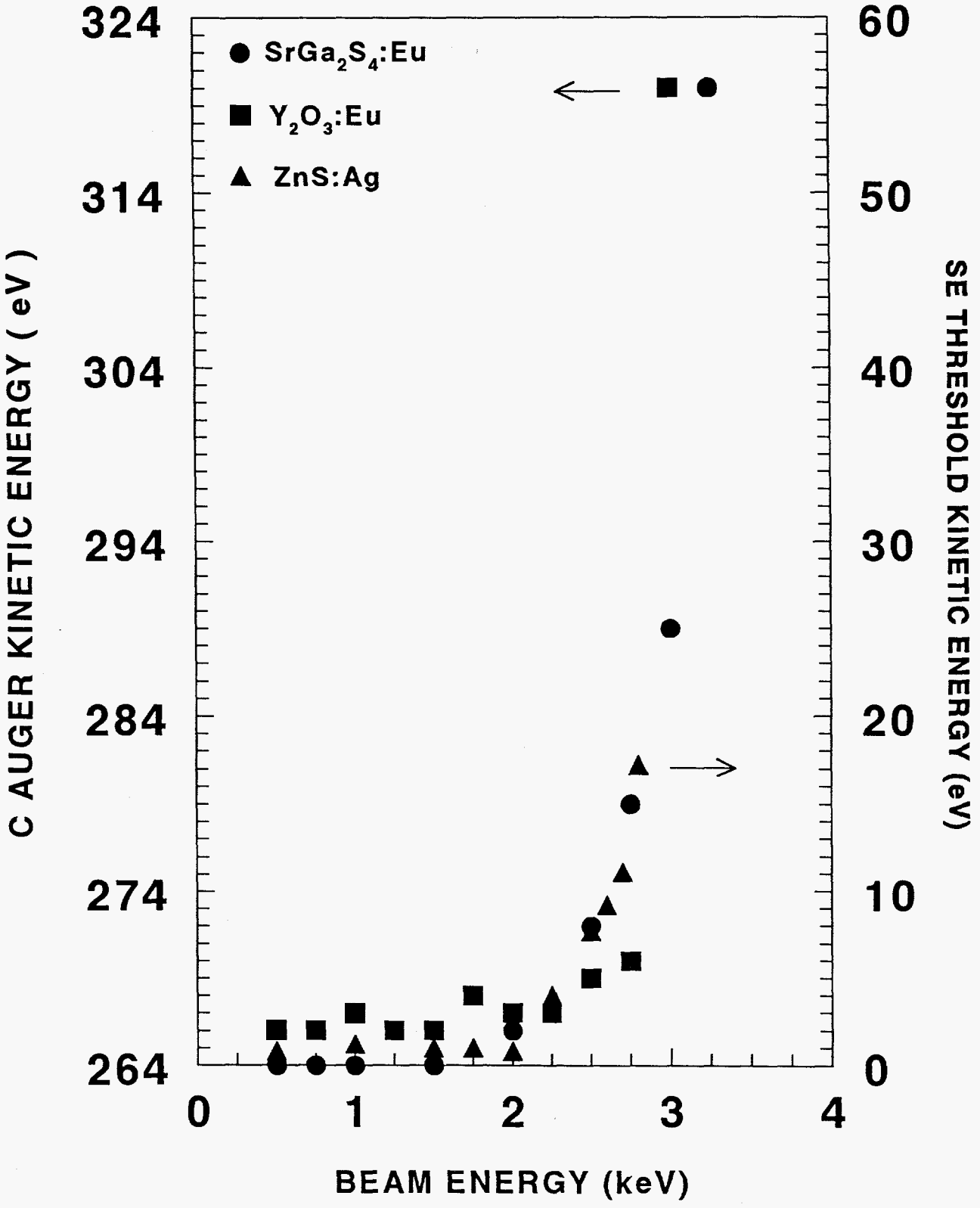

Fig. 2 Seager et al

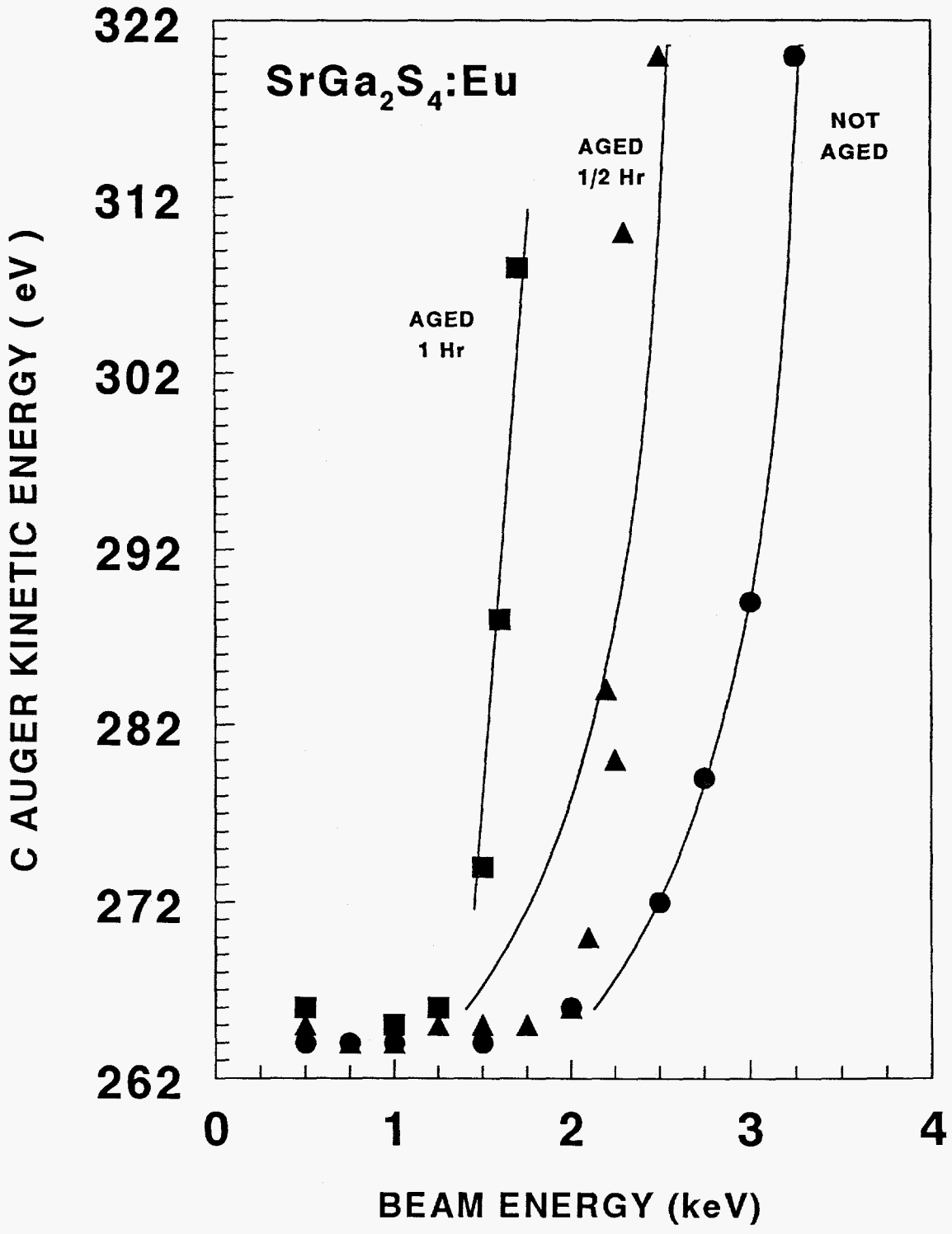

Fig. 3 Seager et al.

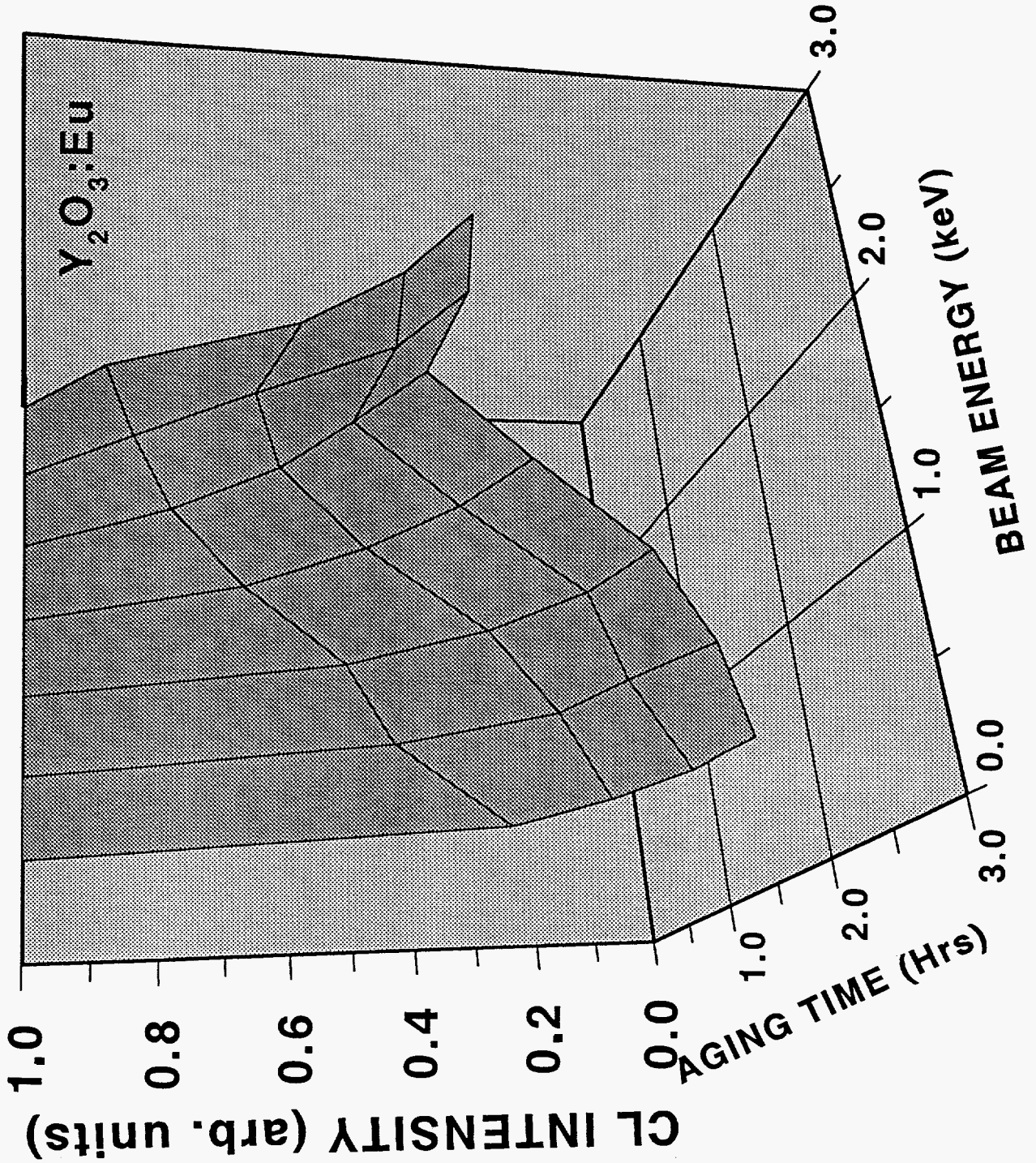

Fig. 4 Seager et al

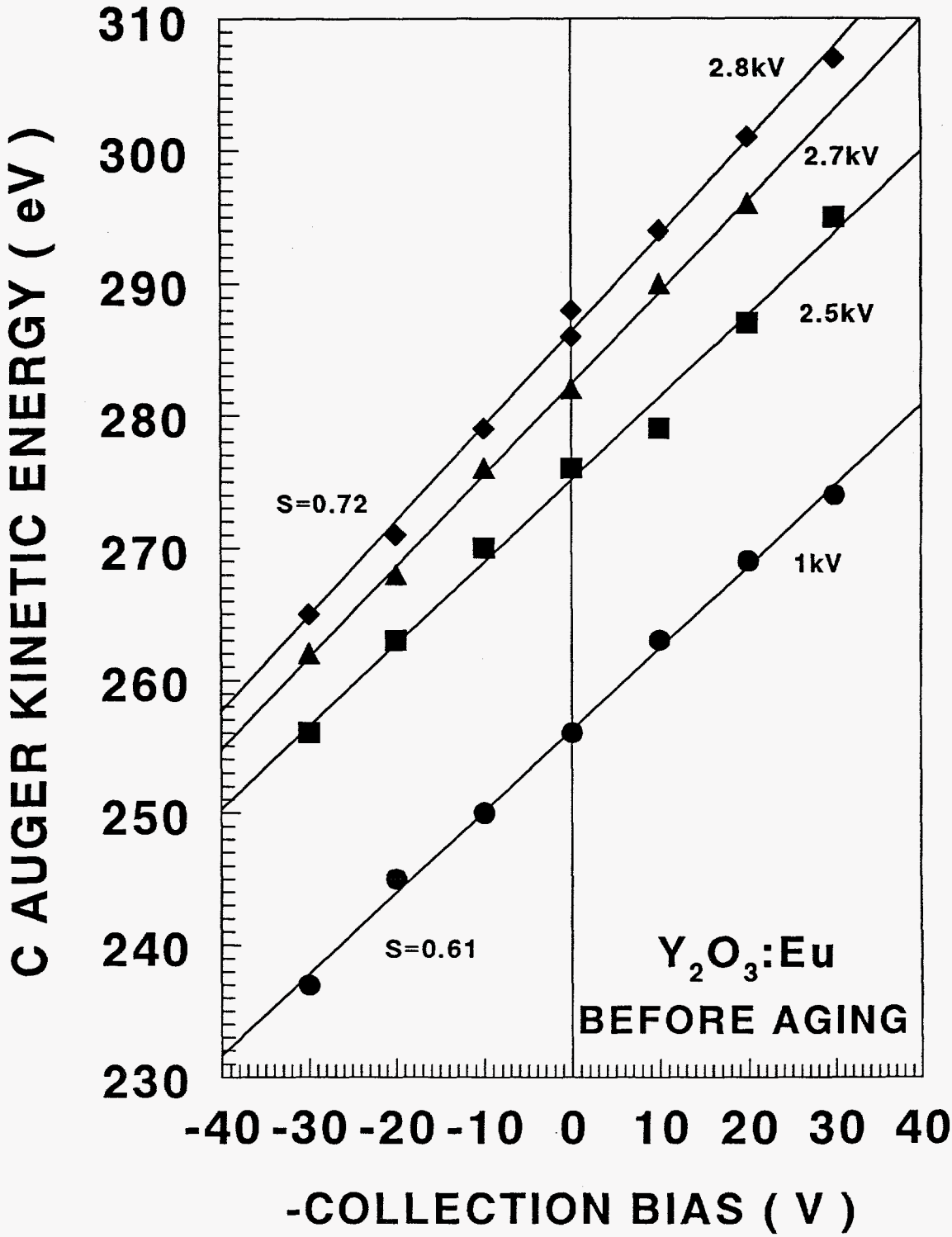

Fig. 5 Seager et al.

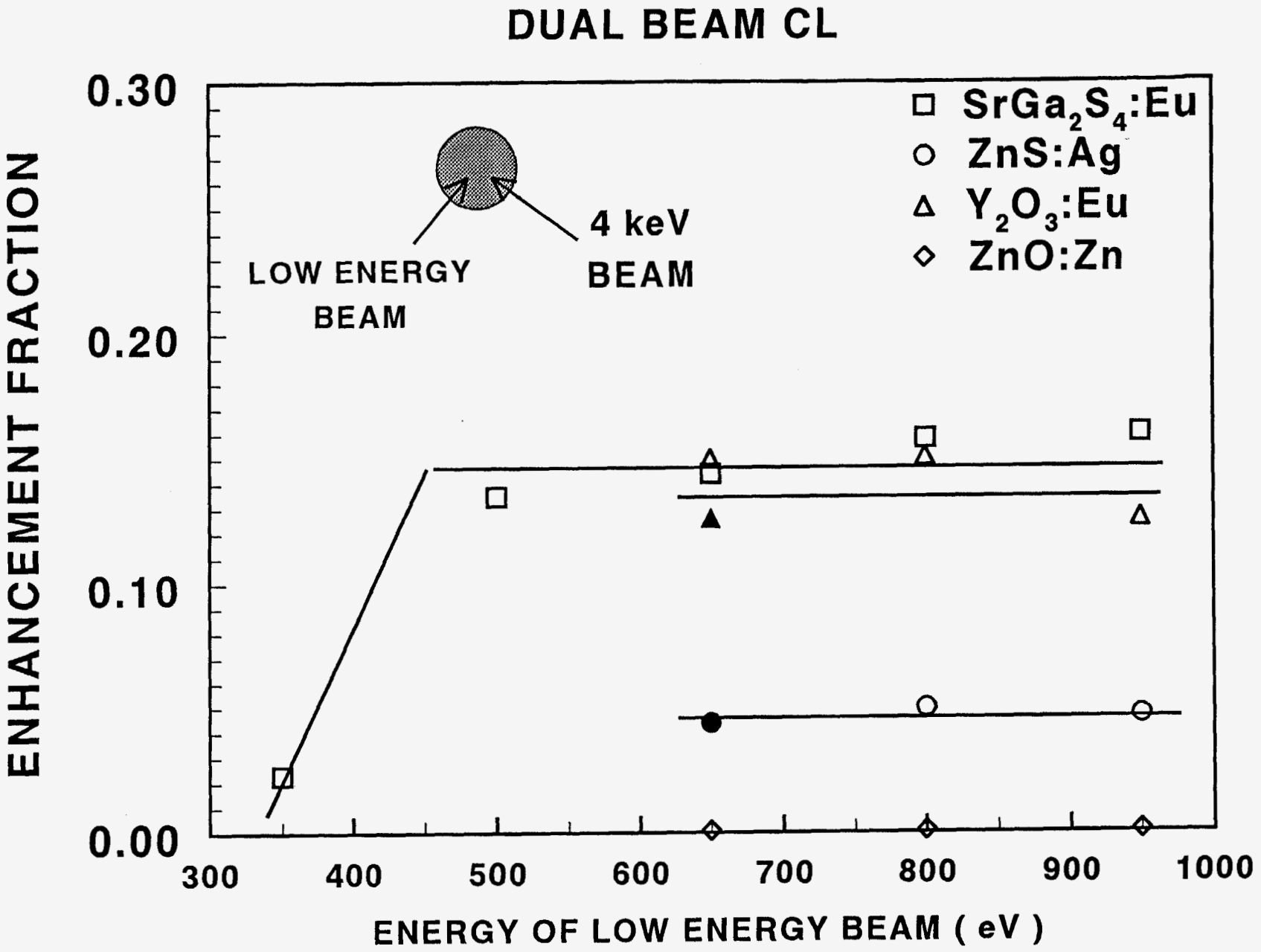

Fig. 6 Seager et al

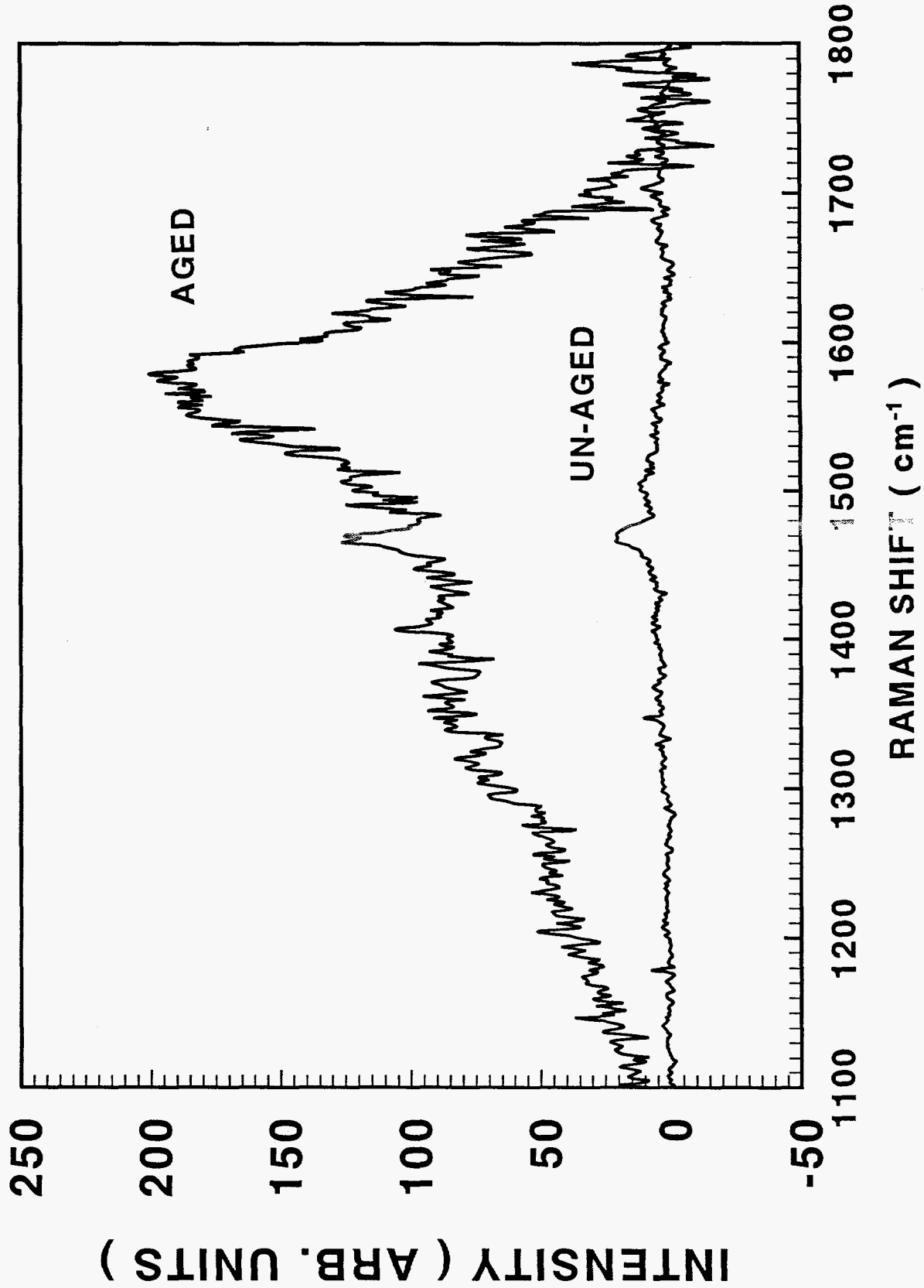

Fig. 7 Seager et al

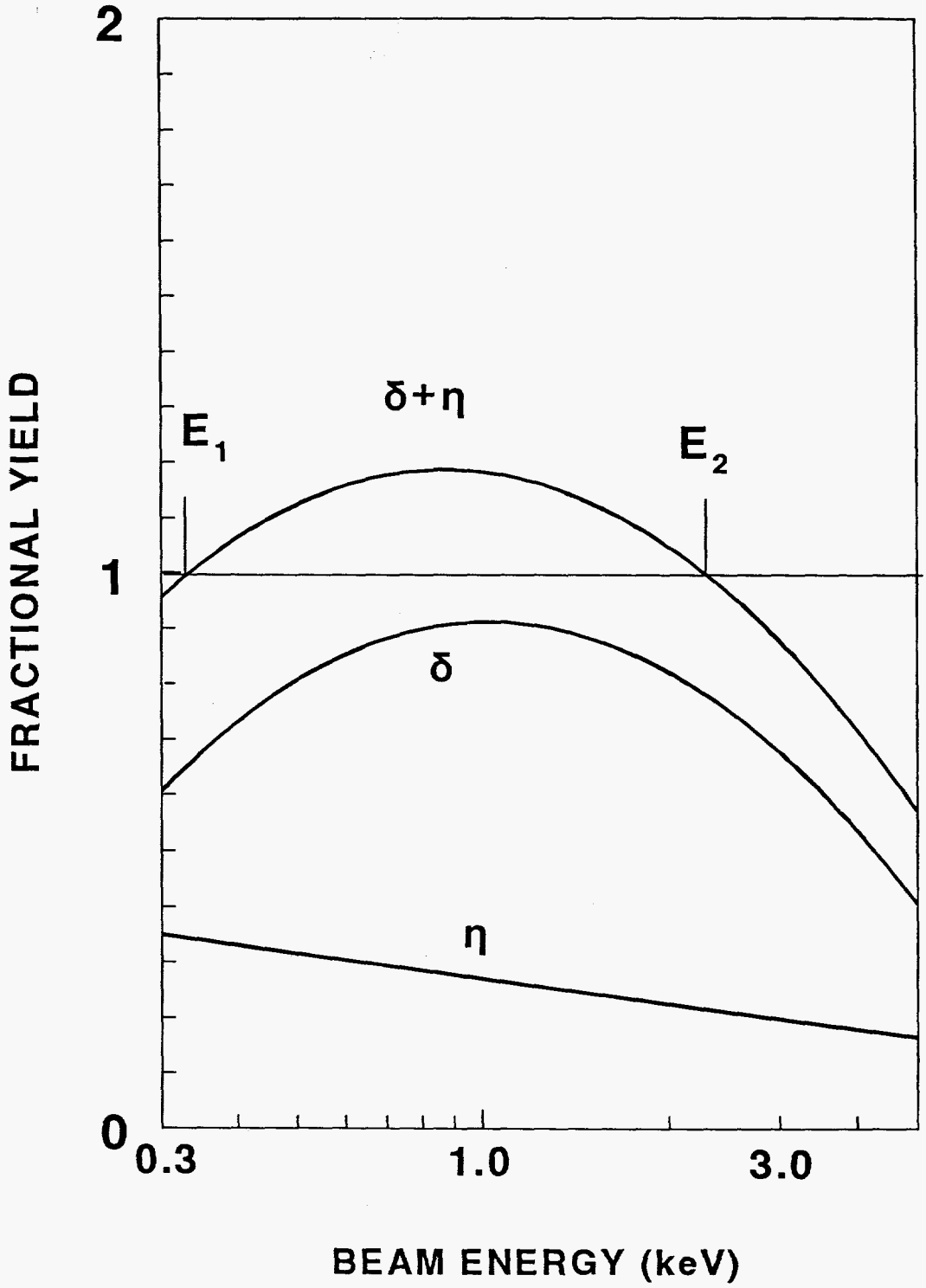

Fig. 8 Seager et al.